TEM STUDY OF NANOSCALE COMPLEXITIES IN THE ZIRCON-REIDITE TRANSFORMATION OCCURRING AT ITS LOWEST-KNOWN SHOCK PRESSURE OF 21.2 GPA. R. Christoffersen[1], T. M. Erickson[1], C. J. Cline II[1], M. J. Cintala[2], Z. Rahman[1] and N. E. Timms[3], [1]Jacobs at NASA Johnson Space Center, 2224 Bay Area Boulevard, Houston, TX, 77058, USA (roy.christoffersen-1@nasa.gov), [2]Astromaterials Research and Exploration Science division, NASA JSC, XI3, 2101 NASA Parkway, Houston, TX, 77058, USA, [3]Space Science and Technology Center, School of Earth and Planetary Science, GPO Box 1984, Perth, WA, 6845, Australia.

Introduction: The high-pressure polymorph of zircon (Zr_2SiO_4) is reidite, a phase with the scheelite structure that was first discovered to form at ca. 12 GPa in static high-pressure experiments [1]. Reidite was subsequently found to occur in naturally shocked zircons from several terrestrial impact localities [2,3], as well as in shock recovery-reverberation experiments performed above 20 GPa [4]. The nature and distribution of reidite occurrences in terrestrial impact localities has pointed to its potential use as a shock pressure indicator, as well as to the importance of understanding its effects on the zircon U-Pb geochronometer [5].

In this study we have used coordinated SEM/Electron Backscatter Diffraction (EBSD) and Field-Emission Scanning Transmission Electron Microscopy (FE-STEM) to study the micro- and nanostructure of reidite and its shocked zircon host produced at 21.2 GPa by experimental shock reverberation [6]. Our results document the TEM-scale nanostructure of reidite formed at 21.2 GPa, a pressure that is significantly lower than observed in previous studies [4]. At these conditions the shocked zircon-reidite assemblage showed diverse microstructures that have not been previously documented at the TEM scale.

Experimental and Analytical Methods: Shock reverberation experiments were performed on oriented single crystals of Mudtank zircon [7] using the flat-plate accelerator (FPA) at NASA Johnson Space Center (JSC) [6]. Single-crystal samples were prepared as ~0.5 mm thick disks ~7 mm in diameter and loaded into a tungsten alloy sample container surrounded by a densely packed aggregate of randomly oriented zircon (< 100 µm) powder. One sample cut normal to <101> was shocked at 18.2 GPa; a second sample cut normal to <001> was shocked at 21.2 GPa. Fragments of the shocked crystals were extracted from the FPA sample container, mounted in epoxy and polished for SEM/EBSD analysis with sub-50 µm colloidal silica.

SEM/EBSD analysis was performed at NASA JSC using a JEOL 7900F field-emission SEM outfitted with an Oxford Instruments Symmetry EBSD detector that also included capabilities for transmitted Kikuchi diffraction (TKD) imaging. Based on SEM/EBSD findings a region in the 21.2 GPa sample was prepared for follow-up TKD and FE-STEM study by focused ion beam (FIB) cross-sectioning using an FEI Quanta Dual-Beam SEM/FIB instrument at NASA JSC. FE-STEM characterization utilized the JEOL 2500SE analytical FE-STEM at NASA JSC. Imaging techniques included both conventional and STEM bright-field (BF)/dark-field (DF) diffraction contrast imaging, and high-resolution lattice fringe imaging (HRTEM).

Results: EBSD analyses of the 18.2 GPa sample found oriented microfractures and crystal-plastic deformation bands but did not detect reidite [6]. EBSD of the 21.2 GPa sample found the same oriented microfractures as the 18.2 GPa sample, but also found prominent cross-cutting lamellar features (1-20 µm wide) that contained sub-micron regions of reidite [6]. TKD phase maps of the 21.2 GPa FIB sample confirmed a heterogeneous distribution reidite in the lamellar features in which it is mixed with regions identified as zircon. Bright-field FE-STEM imaging of the 21.2 GPa FIB section revealed a highly variable range of lamellae widths, with the largest being ~3 µm wide (Fig. 1), but also many 100-500 nm wide lamellae that had not been found by EBSD/TKD mapping at the SEM scale. Although most of the lamellae share a sub-parallel orientation, many of the narrower lamellae form complex closely spaced *en-echelon* sets or are slightly curved (Fig. 1).

The 3 µm-wide lamellar region in the FIB section (arrows; Fig. 1) contains a 300 nm-wide layer of single crystalline reidite along the lamellar margin in contact with the host single-crystal zircon (Fig. 2a). The rest of the region is a polycrystalline assemblage of zircon

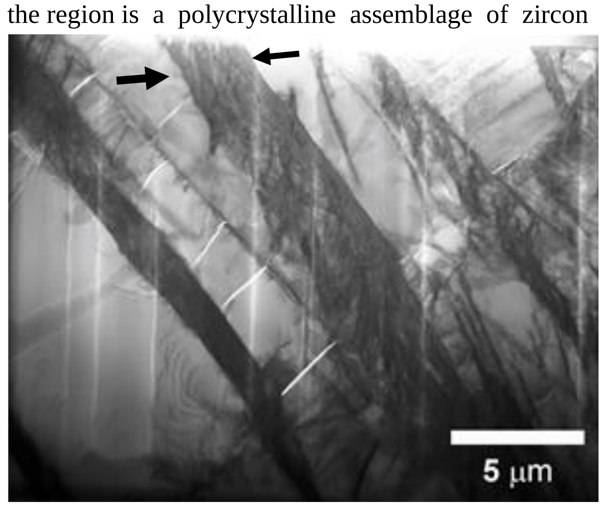

Fig. 1. STEM BF Image of FIB section of 21.2 GPa sample. Arrows show layer described in Fig. 2.

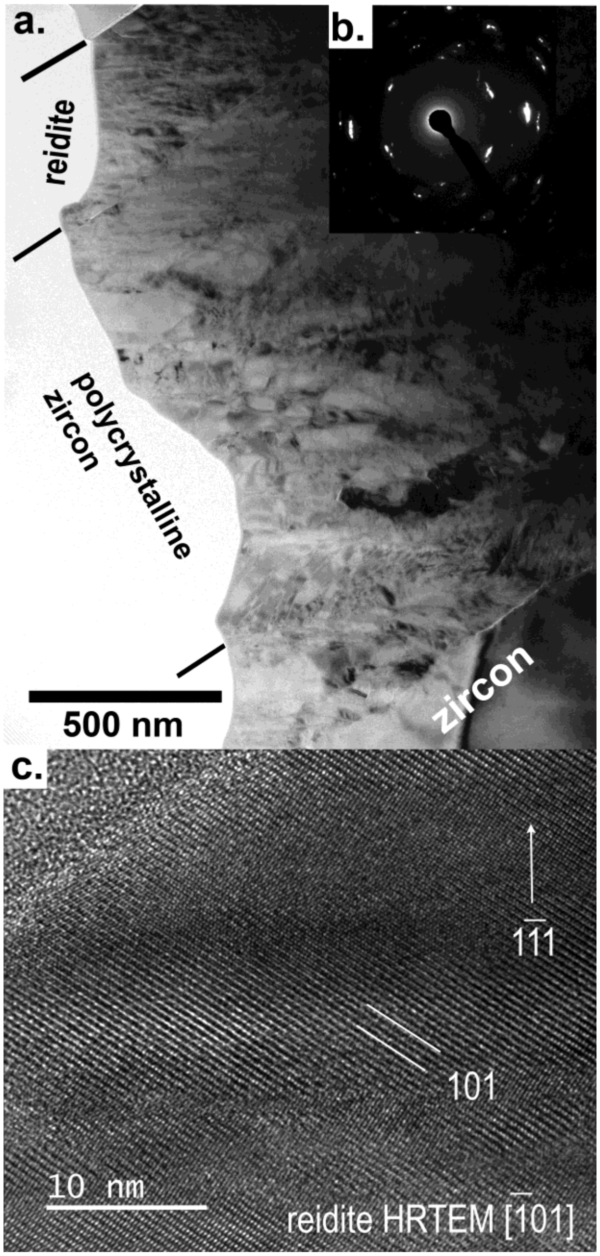

Fig. 2. (a) CTEM BF Image of widest lamellar region in FIB section of 21.2 GPa sample (b) SAED pattern of polycrystalline zircon layer (c) [-101] HRTEM image of reidite single-crystal layer in (a).

grains 20-50 nm across (Fig. 2a). Selected area electron diffraction (SAED) patterns of this assemblage had no indexable reidite reflections (Fig. 2b). The patterns show limited 10-20^o of streaking asterism indicating the zircon grains in the assemblage have a similar crystallographic orientation relative to each other (Fig. 2b). This preferred orientation was confirmed in CTEM DF imaging, which showed the zircon grains forming arrays of oriented, elongate single-crystalline domains. Each domain exhibited dense strain contrast associated with regularly spaced subgrain walls oriented perpendicular to the long axis of the grain. The numerous narrower 100-500 nm wide lamellar features in the FIB sample tend to resemble the polycrystalline portion of the widest layer, being composed of nm-sized zircon crystals with high densities of intra-crystalline defects. Likewise, the limited set SAED patterns obtained from these narrower layers did not contain indexable reidite reflections, and HRTEM images did not show reidite lattice fringes. The un-transformed zircon crystal in between the lamellar regions contains {112} mechanical twins that tend to be concentrated in the highly deformed regions along lamellar boundaries with the host zircon.

HRTEM images of the single-crystalline reidite layer in the ~3 µm-wide lamellar region exhibit a wavy contrast modulation oriented normal to the $1\bar{1}1$ reciprocal lattice direction. The modulation is associated with regularly spaced crystallographic boundaries that we suspect may be inclined {112} micro twins as found in [4].

Discussion: Our FE-STEM results corroborate our previous EBSD identification of reidite within the shock-deformed lamellar regions of the 21.2 GPa sample [6]. It is not necessarily a given, however, that all these lamellar regions contain enough reidite to consistently show up in SAED patterns or HRTEM images. The lamellar regions are better characterized as zones of concentrated brittle-plastic deformation in which the microstructure suggests a strong shear component. More detailed study is needed to fully determine the presence or absence of reidite in these nm-scale lamellar regions. The consistent indexing of reidite in EBSD phase maps of the widest (10-30 µm) lamellae at the SEM scale, and localization of well-formed single-crystalline reidite to the widest lamellar region in the TEM FIB sample suggests these wider lamellae may define zones of more efficient reidite formation, possibly due to higher localized shear deformation. The 21.2 GPa shock reverberation transition pressure reported here and in [6] is likely higher than the transition pressure that would correspond to single-shock conditions in natural impacts.

References: [1] Reid A. F. and Ringwood A. E. (1969) EPSL, 6, 205-208. [2] Glass B. P. et al. (2002) *Am. Min.*, 87, 562-565. [3] Erickson T. M. et al. (2017) *Con. Min. Pet.*, 172. [4] Leroux H. et al. (1999) *EPSL, 169*, 291 – 301. [5] Erickson T. M. et al. (2021 GCA, 304, 68. [6] Erickson T. M. et al. (2020) *51st LPSC, Abstract #1581*. [7] Black L. P. & Gulson B. L. (1978) *J. of Aus. Geo. and Geophys*. 3, 277 – 232.